
Balancing Privacy and Security in Federated Learning with FedGT: A Group Testing Framework

Marvin Xhemrishi¹ Johan Östman² Antonia Wachter-Zeh¹ Alexandre Graell i Amat³

¹ Technical University of Munich ² AI Sweden ³ Chalmers University of Technology

Abstract

We propose FedGT, a novel framework for identifying malicious clients in federated learning with secure aggregation. Inspired by group testing, the framework leverages overlapping groups of clients to detect the presence of malicious clients in the groups and to identify them via a decoding operation. The identified clients are then removed from the training of the model, which is performed over the remaining clients. FedGT strikes a balance between privacy and security, allowing for improved identification capabilities while still preserving data privacy. Specifically, the server learns the aggregated model of the clients in each group. The effectiveness of FedGT is demonstrated through extensive experiments on the MNIST and CIFAR-10 datasets, showing its ability to identify malicious clients with low misdetection and false alarm probabilities, resulting in high model utility.

1 Introduction

Federated learning [1] is a distributed machine learning paradigm that enables multiple devices (clients) to collaboratively train a machine learning model under the orchestration of a central server while preserving the privacy of their raw data. To provide privacy, the clients share their local models instead of the raw data with the central server.

In its original form, federated learning is prone to model-inversion attacks [2, 3], which allow the central server to infer clients' data from their local model updates. To prevent such attacks, secure aggregation protocols [4, 5] have been proposed. These protocols ensure that the server only observes the aggregate of the client models instead of individual models.

A salient problem in federated learning is poisoning attacks [6], where faulty and/or malicious clients corrupt the jointly-trained global model by introducing mislabeled training data (*data poisoning*) [7, 8], or by modifying local model updates (*model poisoning*) [9]. Poisoning attacks represent a serious security risk for critical applications, and require effective mitigation strategies to ensure the integrity and accuracy of the trained models. Several protocols have been proposed to provide resiliency against poisoning attacks [10], including robust aggregation [11, 12, 13], ensemble-based methods [14], and schemes relying on a server dataset [15, 16, 17, 18]. However, these protocols require access to the clients' individual models and are therefore vulnerable to model-inversion attacks. Addressing resiliency against poisoning attacks and devising protocols for the identification of malicious clients in federated learning with secure aggregation remains a significant challenge [19]. Specifically, secure aggregation protocols protect the privacy of clients at the expense of camouflaging adversaries. Hence, there is a fundamental trade-off between security and privacy.

In this paper, we propose FedGT, a novel framework for identifying malicious clients in federated learning with secure aggregation. Our framework is inspired by group testing [20], a paradigm to detect defective items in a large population that significantly reduces the required number of tests compared to the naive approach of testing each item individually. FedGT's key idea is to group clients

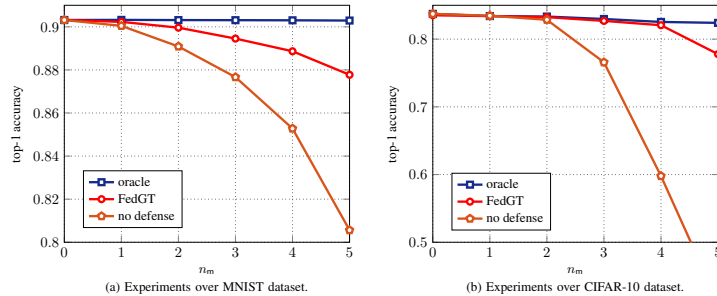


Figure 1: Average top-1 accuracy versus the number of malicious clients.

into overlapping groups. For each group, the central server observes the aggregated model of the clients and runs a suitable test to detect the presence of malicious clients in the group. The malicious clients are then identified through a decoding operation, allowing their removal from the training of the global model. FedGT trades-off client’s data privacy, provided by secure aggregation, with *security*, understood here as the ability to identify malicious clients: It encompasses security-oriented methods, e.g., robust aggregation techniques, and privacy-oriented methods, e.g., secure aggregation, by selecting group sizes of one and the total amount of clients, respectively. However, by allowing group sizes between these two extremes, FedGT strikes a balance between privacy and security, i.e., improved identification capabilities comes at the cost of secure aggregation involving fewer clients.

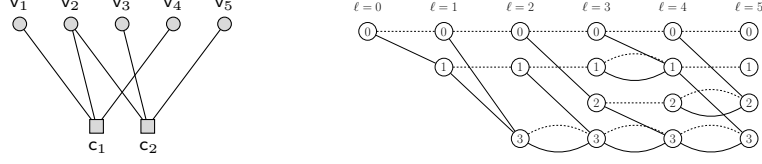
We demonstrate FedGT’s effectiveness in identifying malicious clients through extensive experiments for a classification problem on the MNIST and CIFAR-10 datasets under data-poisoning untargeted and targeted attacks. Fig. 1 illustrates the performance of FedGT for a scenario with 15 clients (typical of a cross-silo federated learning) and an untargeted attack. The figure shows the top-1 accuracy after 10 (MNIST) and 50 (CIFAR-10) communication rounds, respectively, versus the number of malicious clients n_m . When no defense is in place, a significant drop in accuracy is observed as the number of malicious clients grows. Remarkably, FedGT permits to identify malicious clients with low misdetection and false alarm probabilities, which translates into a high accuracy.

2 Related work

To the best of our knowledge, only the works [21, 22, 23] address resiliency against poisoning attacks in conjunction with secure aggregation. The work [21] is the first single-server solution to account for both privacy and security in federated learning. The protocol is based on drop-out resilient secure aggregation where the server utilizes secret sharing to first obtain the pairwise Euclidean distance between the clients’ updates and then selects what clients to aggregate by means of multi-Krum [11]. However, it is not clear if the pairwise differences can leak extra information. In [22], a robust aggregation protocol based on an approximate geometric median (computed exploiting secure aggregation) is proposed. However, from the geometric median, one is unable to identify malicious clients and the protocol is known to deteriorate the performance compared to many alternative robust aggregation techniques [24]. The work [23] presents a privacy-preserving tree-based robust aggregation method. In particular, each leaf in the tree consists of a subgroup of clients who securely aggregate their local models. To achieve privacy between subgroups, masking is done on all but the last parameters in the aggregated models. By using the Euclidean distance between the unmasked parameters and the corresponding parameters in the global model, an outlier removal scheme, based on variance thresholding, is used iteratively to determine what groups should contribute to the global model. The approach in [23] is the method closest to ours as it relies on dividing clients into subgroups and on testing the group aggregates. However, contrary to FedGT, the method in [23] is unable to identify malicious clients and is not able to leverage the information of overlapping groups.

3 Preliminaries

Group testing. Group testing [20, 25] encompasses a family of test schemes aiming at identifying items affected by some particular condition, usually called *defective* items (e.g., individuals infected by a virus), among a large population of n items (e.g., all individuals). The overarching goal of group testing is to design a testing scheme such that the number of tests needed to identify the defective items is minimized. The principle behind group testing is that, if the number of defective items



(a) Circles represent VNs, squares CNs (b) Dashed edges represent a “0”, solid edges a “1”
 Figure 2: Bipartite graph (left) and trellis (right) representation of the assignment matrix \mathbf{A} in (1).

is significantly smaller than n , then negative tests on groups (or pools) of items can spare many individual tests. Following this principle, the items are grouped into overlapping groups, and tests are performed on each group. Based on the test results on the groups, the defective items can then be identified—in general with some probability of error—via a decoding operation.

Attack model. We consider a scenario with n clients out of which n_m are compromised (referred to as *malicious* clients). A client may be compromised due to hardware malfunction or adversarial corruption. In the latter case, we assume that the malicious clients can collude and therefore perform coordinated attacks against the global model. In this paper, we restrict ourselves to data-poisoning attacks, which constitute the most realistic type of attacks for cross-silo federated learning [26].

4 FedGT: Group testing for federated learning with secure aggregation

We consider a population of n clients, n_m of which are malicious. We define the *defective vector* $\mathbf{d} = (d_1, d_2, \dots, d_n)$ with entries representing whether a client is malicious or not. In particular, $d_i = 1$ if client i is malicious and $d_i = 0$ if it is not. Hence, it follows that $\sum_{i=1}^n d_i = n_m$. Note that \mathbf{d} is unknown, i.e., we do not know a priori which clients are malicious.

Before performing federated learning with secure aggregation, the server attempts to identify the malicious clients, which are then excluded from the training, as explained next.

Borrowing ideas from group testing [20], the n clients are grouped into m overlapping *test groups*. We denote by $\mathcal{P}_1, \mathcal{P}_2, \dots, \mathcal{P}_m$ the set of indices of the clients belonging to test group j , i.e., if client i is a member of test group j , then $i \in \mathcal{P}_j$. The assignment of clients to test groups can be described by an assignment matrix $\mathbf{A} = (a_{i,j}), i \in [m], j \in [n]$, where $a_{i,j} = 1$ if client j participates in test group i and $a_{i,j} = 0$ otherwise. Further, the assignment of clients to test groups, i.e., matrix \mathbf{A} , can be conveniently represented by a bipartite graph consisting of n *variable nodes* (VNs) v_1, \dots, v_n corresponding to the n clients, and m *constraint nodes* (CNs) c_1, \dots, c_m , corresponding to the m tests. An edge between VN v_j and CN c_i is then drawn if client j participates in test group i , i.e., if $a_{i,j} = 1$. The bipartite graph corresponding to a scenario with 5 clients and 2 test groups with assignment matrix

$$\mathbf{A} = \begin{pmatrix} 1 & 1 & 0 & 1 & 0 \\ 0 & 1 & 1 & 0 & 1 \end{pmatrix} \quad (1)$$

is depicted in Fig. 2a. Matrix \mathbf{A} and hence the corresponding bipartite graph is a design choice.

FedGT is such that, for each test group, the central server only observes the aggregate of the models of the clients in the group. The central server then applies a suitable test to the aggregate model for each test group to identify the presence of malicious clients in the group. We remark that the proposed framework is general and can be applied to any test on the test group aggregates. Let $t_i, i \in [m]$, be the result of the test for test group i , where $t_i = 1$ if the test is positive and $t_i = 0$ if the test is negative. We collect the result of the m tests into the binary vector $\mathbf{t} = (t_1, t_2, \dots, t_m)$.

We define the syndrome vector $\mathbf{s} = (s_1, \dots, s_m)$, where $s_i = 1$ if at least one client participating in test group i is malicious and $s_i = 0$ if no client participating in test group i is malicious, i.e.,

$$s_i = \bigvee_{j \in \mathcal{P}_i} d_j \quad \text{and} \quad \mathbf{s} = \mathbf{d} \vee \mathbf{A}^\top.$$

For perfect (non-noisy) test results, it follows that $\mathbf{t} = \mathbf{s}$. However, note that the result of a test may be erroneous, i.e., the result of the test may be $t_i = 1$ even if no malicious clients are present or $t_i = 0$ even if malicious clients are present. In general, the (noisy) test vector \mathbf{t} is statistically dependent on the syndrome vector \mathbf{s} according to an (unknown) probability distribution $Q(\mathbf{t}|\mathbf{s})$.

Given the test results \mathbf{t} and the assignment matrix \mathbf{A} , the goal is to identify the malicious clients, i.e., infer the defective vector \mathbf{d} . The design of the assignment matrix \mathbf{A} and the corresponding inference problem is akin to an error-correcting coding problem, where the assignment matrix \mathbf{A} can be seen as the parity-check matrix of a code, and the inference problem corresponds to a decoding operation based on \mathbf{A} and \mathbf{t} . Thus, a suitable choice for \mathbf{A} is the parity-check matrix of a powerful error-correcting code, i.e., with good distance properties. Furthermore, \mathbf{d} can be inferred applying conventional decoding techniques. We denote by $\hat{\mathbf{d}} = (\hat{d}_1, \dots, \hat{d}_n)$ the estimated defective vector provided by the decoding operation, and define $\mathcal{D} = \{i : \hat{d}_i = 1\}$. Once obtained $\hat{\mathbf{d}}$, FedGT excludes clients $i \in \mathcal{D}$ from the training and performs secure aggregation on the remaining—flagged non-malicious—clients.

The performance of FedGT, measured in terms of the utility of the model, is affected by two quantities: the miss-detection probability, i.e., the probability that a client is flagged as non-malicious while it is, and the false-alarm probability, i.e., the probability that a client is flagged as malicious while it is not, defined as

$$P_{\text{MD}} \triangleq \frac{1}{n} \sum_{i=1}^n \Pr(\hat{d}_i = 0 | d_i = 1), \quad P_{\text{FA}} \triangleq \frac{1}{n} \sum_{i=1}^n \Pr(\hat{d}_i = 1 | d_i = 0).$$

A high miss-detection probability will result in many malicious clients poisoning the global model, hence yielding poor utility, while a high false-alarm probability will result in excluding many non-malicious clients from the training, thereby also impairing the utility. The miss-detection and false-alarm probabilities depend in turn on the assignment matrix \mathbf{A} , the decoding strategy, and the nature of the test performed. We discuss the decoding strategy to estimate \mathbf{d} in Section 5.

4.1 Privacy-security trade-off and the choice of assignment matrix \mathbf{A}

Vanilla federated learning [1] and federated learning with *full* secure aggregation [4] can be seen as the two extreme cases of the proposed framework, corresponding to n (non-overlapping) groups and a single group with n clients, respectively. In vanilla federated learning, tests on individual models can be performed, making it easier to identify malicious clients at the expense of clients' privacy. In contrast, full secure aggregation provides privacy by enabling the server to observe only the aggregation of the n models. However, it does not allow for the identification of malicious clients.

Under FedGT, the server observes m aggregated models $\mathbf{u}_1 \dots, \mathbf{u}_m$, with $\mathbf{u}_i = \sum_{j=1}^n a_{i,j} \mathbf{c}_j$ and \mathbf{c}_j being the local model of client j . The privacy of the clients increases with the number of models aggregated [27]. Hence, FedGT trades privacy for providing security, i.e., identification of the malicious clients. Furthermore, due to the aggregates being from overlapping groups, there might be additional privacy loss. This loss depends on the assignment matrix \mathbf{A} . Specifically, due to the overlapping groups, there might exist a vector $\mathbf{b} \in \mathbb{R}^m$ such that $\sum_{i=1}^m b_i \mathbf{u}_i = \mathbf{c}_j$ for some $j \in [n]$, or equivalently $\mathbf{b}\mathbf{A} = \mathbf{e}_j$, where \mathbf{e}_j is the j -th unit vector. This will occur if $\mathbf{e}_j \in \text{Sp}_r(\mathbf{A})$, where $\text{Sp}_r(\mathbf{A})$ is the row span of \mathbf{A} . Generally speaking, for a subset $\mathcal{R} \subset [n]$ of cardinality r , if $\sum_{l \in \mathcal{R}} f_l \mathbf{e}_l \in \text{Sp}_r(\mathbf{A})$ where $f_l \neq 0$, there exists a vector \mathbf{b}' such that $\sum_{i=1}^m b'_i \mathbf{u}_i = \sum_{l \in \mathcal{R}} f_l \mathbf{c}_l$. Thus, we conclude that FedGT achieves the same privacy as a secure aggregation scheme with $r < n$ clients, where r is the smallest non-zero cardinality of the subset \mathcal{R} . In other words, r is the smallest non-zero Hamming weight of the vectors in the row span of \mathbf{A} , or in the coding theory jargon, the minimum Hamming distance of the code generated by \mathbf{A} as its generator matrix.

The assignment matrix \mathbf{A} should be carefully chosen to optimize the trade-off between privacy and security: To improve identification of malicious clients, one should choose \mathbf{A} as the parity-check matrix of an error-correcting code with good distance properties, while to achieve a high privacy level, \mathbf{A} should correspond to the generator matrix of a code of large minimum Hamming distance.

5 Decoding: inferring the defective vector \mathbf{d}

Several decoding techniques can be applied to infer \mathbf{d} . In this paper, we consider optimal inference in a Neyman-Pearson sense, which prescribes for some $\Delta' > 1$

$$\hat{d}_i = \begin{cases} 0 & \text{if } \Pr(\mathbf{t} | d_i = 0) > \Pr(\mathbf{t} | d_i = 1) \Delta' \\ 1 & \text{if } \Pr(\mathbf{t} | d_i = 0) < \Pr(\mathbf{t} | d_i = 1) \Delta' \end{cases}.$$

The Neyman-Pearson criterion can be rewritten in terms of the log-likelihood ratio (LLR) $L_i = \log(\Pr(\mathbf{t}|d_i = 0)/\Pr(\mathbf{t}|d_i = 1))$ as

$$\hat{d}_i = \begin{cases} 0 & \text{if } L_i > \Delta \\ 1 & \text{if } L_i < \Delta \end{cases}, \quad (2)$$

where $\Delta = \log(\Delta')$. Further, we can write the LLR L_i as

$$L_i = \log\left(\frac{\Pr(d_i = 0|\mathbf{t})}{\Pr(d_i = 1|\mathbf{t})}\right) - \log\left(\frac{\Pr(d_i = 0)}{\Pr(d_i = 1)}\right) = L_i^{\text{APP}} - \log\left(\frac{1-\delta}{\delta}\right), \quad (3)$$

where δ is the *prevalence* of malicious clients in the population of n clients, i.e., the probability of a client being malicious, $\delta = \Pr(d_i = 1)$. In a frequentist approach to probability, $\delta = n_m/n$. Using (3), the Neyman-Pearson criterion in (2) can be rewritten in terms of the a posteriori LLR L_i^{APP} as

$$\hat{d}_i = \begin{cases} 0 & \text{if } L_i^{\text{APP}} > \Lambda \\ 1 & \text{if } L_i^{\text{APP}} < \Lambda \end{cases}, \quad (4)$$

where $\Lambda = \Delta + \log\left(\frac{1-\delta}{\delta}\right)$. Note that, as Λ increases, P_{FA} increases and P_{MD} decreases.

The Neyman-Pearson criterion requires the computation of the a posteriori LLRs L_i^{APP} . For not-too-large matrices \mathbf{A} , the a posteriori LLRs can be computed efficiently via the forward-backward algorithm [28], which exploits the trellis representation of the assignment matrix \mathbf{A} . For large matrices \mathbf{A} , the computation of the a posteriori LLRs is not feasible, and one needs to resort to suboptimal decoding strategies, such as belief propagation [29], a message passing decoding algorithm for codes on graphs based on the exchange of messages over the edges of the bipartite graph representation of the code (in our scenario, the bipartite graph corresponding to \mathbf{A} , see Fig. 2a).

In Subsection 5.1, we describe how to obtain the trellis diagram corresponding to a given assignment matrix \mathbf{A} , and in Subsection 5.2, we discuss the forward-backward algorithm to compute the a posteriori LLRs to infer \mathbf{d} .

5.1 Trellis representation of assignment matrix \mathbf{A}

In this section, we describe the trellis representation corresponding to assignment matrix \mathbf{A} , which can be used to compute the a posteriori LLRs as described in Section 5.2. The trellis representation was originally introduced for linear block codes in [30] and applied to group testing in [31].

For a given defective vector $\tilde{\mathbf{d}}$ (not necessarily the true one), define the *syndrome vector* $\tilde{\mathbf{s}} = (\tilde{s}_1, \dots, \tilde{s}_n)$, where \tilde{s}_i is given by $\tilde{s}_i = \bigvee_{j \in \mathcal{P}_i} \tilde{d}_j$, where \bigvee is the logical disjunction. The syndrome vector can be written as a function of the defective vector $\tilde{\mathbf{d}}$ and the assignment matrix as $\tilde{\mathbf{s}} = \tilde{\mathbf{d}} \vee \mathbf{A}^T$. Note that several defective vectors are compatible with a given syndrome $\tilde{\mathbf{s}}$. Let \mathcal{D} be the set of all possible defective vectors, i.e., all binary tuples of length n . We denote by $\mathcal{D}_{\tilde{\mathbf{s}}}$ the set of defective vectors compatible with syndrome vector $\tilde{\mathbf{s}}$, i.e., $\mathcal{D}_{\tilde{\mathbf{s}}} = \{\tilde{\mathbf{d}} \in \mathcal{D} : \tilde{\mathbf{d}} \vee \mathbf{A}^T = \tilde{\mathbf{s}}\}$.

Let \mathbf{a}_j be the j -th column of matrix \mathbf{A} . The syndrome corresponding to defective vector $\tilde{\mathbf{d}}$ can then be rewritten as $\tilde{\mathbf{s}} = \bigvee_{i=1}^n (\tilde{d}_i \wedge \mathbf{a}_i^T)$, where \wedge is the logical conjunction operator. This equation naturally leads to a trellis representation of the assignment matrix \mathbf{A} as explained next. A trellis is a graphical way to represent matrix \mathbf{A} , consisting of a collection of nodes connected by edges. The trellis corresponding to matrix in (1) is depicted in Fig. 2b. Horizontally, the nodes, called trellis states, are grouped into sets indexed by parameter $\ell \in \{0, \dots, n\}$, referred to as the trellis depth.

Let $\tilde{\mathbf{s}}_\ell$ be the *partial syndrome vector* at trellis depth $\ell \in [n]$ corresponding to $\tilde{\mathbf{d}}$, given as $\tilde{\mathbf{s}}_\ell = \bigvee_{i=1}^\ell (\tilde{d}_i \wedge \mathbf{a}_i^T)$. It is easy to see that $\tilde{\mathbf{s}}_\ell$ can be obtained from $\tilde{\mathbf{s}}_{\ell-1}$ as $\tilde{\mathbf{s}}_\ell = \tilde{\mathbf{s}}_{\ell-1} \vee (\tilde{d}_\ell \wedge \mathbf{a}_\ell^T)$, with $\tilde{\mathbf{s}}_0$ being the all-zero vector. The trellis representation is such that each state in the trellis represents a particular partial syndrome. The trellis is then constructed as follows: At trellis depth $\ell = 0$ there is a single trellis state corresponding to $\tilde{\mathbf{s}}_0$. At trellis depth $\ell \in [n]$, the trellis states correspond to all possible partial syndrome vectors $\tilde{\mathbf{s}}_\ell$ for all possible partial syndrome vectors $(\tilde{d}_1, \dots, \tilde{d}_\ell)$, with $\tilde{d}_i \in \{0, 1\}$. For example, at trellis depth $\ell = 1$ there are only two trellis states, corresponding to partial syndromes $0 \wedge \mathbf{a}_1^T = (0, \dots, 0)$ and $1 \wedge \mathbf{a}_1^T = (a_{1,1}, \dots, a_{1,m})$, i.e., for $\tilde{d}_1 = 0$ and $\tilde{d}_1 = 1$,

respectively. Note that at trellis depth $\ell = n$, there are 2^m trellis states, corresponding to all possible syndromes \tilde{s} . For simplicity, we label the trellis state corresponding to partial syndrome vector $\tilde{s}_\ell = (s_{\ell,1}, \dots, s_{\ell,m})$ by its decimal representation $\sum_{i=1}^m \tilde{s}_{\ell,i} 2^{i-1}$. Finally, an edge from the node at trellis depth ℓ corresponding to partial syndrome \tilde{s}_ℓ to the node at trellis depth $\ell + 1$ corresponding to partial syndrome $\tilde{s}_{\ell+1}$ is drawn if $\tilde{s}_{\ell+1} = \tilde{s}_\ell \vee (\tilde{d}_{\ell+1} \wedge \mathbf{a}_{\ell+1}^\top)$, with $\tilde{d}_{\ell+1} \in \{0, 1\}$. The edge is labeled by the value of $\tilde{d}_{\ell+1}$ enabling the transition between \tilde{s}_ℓ and $\tilde{s}_{\ell+1}$.

Example 5.1. For the trellis of Fig. 2b, corresponding to the assignment matrix in (1) with $n = 5$ nodes and $m = 2$ tests, the number of trellis states at trellis depth $\ell = 5$ is $2^2 = 4$, i.e., all length-2 binary vectors (in decimal notation $\{0, 1, 2, 3\}$). At trellis depth $\ell = 2$, there are three states, corresponding to all possible partial syndromes $\tilde{s} = \bigvee_{i=1}^2 (\tilde{d}_i \wedge \mathbf{a}_i^\top)$, i.e., all possible (binary) linear combinations of the two first columns of matrix \mathbf{A} in (1), resulting in states $(0, 0) \vee (0, 0) = (0, 0) = 0$, $(0, 0) \vee (1, 1) = (1, 1) = 3$, $(1, 0) \vee (0, 0) = (1, 0) = 1$, and $(1, 0) \vee (1, 1) = (1, 1) = 3$.

The trellis graphically represents all possible defective vectors $\tilde{\mathbf{d}}$ and their connection to the syndromes $\tilde{\mathbf{s}}$ via the assignment matrix \mathbf{A} . In particular, the paths along the trellis originating in the all-zero state at trellis depth $\ell = 0$ and ending in trellis state $\tilde{\mathbf{s}}$ at trellis depth $\ell = n$ correspond to all defective vectors $\tilde{\mathbf{d}}$ compatible with syndrome $\tilde{\mathbf{s}}$.

5.2 The forward-backward algorithm

The a posteriori LLRs can be computed efficiently using the trellis representation of matrix \mathbf{A} introduced in the previous subsection via the forward-backward algorithm [28].

Let $\mathcal{E}_\ell^{(0)}$ and $\mathcal{E}_\ell^{(1)}$ be the set of edges connecting trellis states at trellis depth $\ell - 1$ with states at trellis depth ℓ labeled by $\tilde{d}_\ell = 0$ and $\tilde{d}_\ell = 1$, respectively. L_ℓ^{APP} can be computed as

$$L_\ell^{\text{APP}} = \log \sum_{(\sigma', \sigma) \in \mathcal{E}_\ell^{(0)}} \alpha_{\ell-1}(\sigma') \gamma(\sigma', \sigma) \beta_\ell(\sigma) - \log \sum_{(\sigma', \sigma) \in \mathcal{E}_\ell^{(1)}} \alpha_{\ell-1}(\sigma') \gamma(\sigma', \sigma) \beta_\ell(\sigma), \quad (5)$$

where (σ', σ) denotes an edge connecting state σ' at trellis depth $\ell - 1$ with state σ at trellis depth ℓ .

The quantities $\alpha_{\ell-1}(\sigma')$ and $\beta_\ell(\sigma)$ are called the forward and backward metrics, respectively, and can be computed using the recursions

$$\alpha_\ell(\sigma) = \sum_{\sigma'} \alpha_{\ell-1}(\sigma') \gamma_\ell(\sigma', \sigma), \quad \beta_{\ell-1}(\sigma') = \sum_{\sigma} \beta_\ell(\sigma) \gamma_\ell(\sigma', \sigma),$$

with initialization of the forward recursion $\alpha_0(0) = 1$ and of the backward recursion $\beta_n(\sigma) = Q(\mathbf{t} | \mathbf{s}(\sigma))$, where $\mathbf{s}(\sigma)$ is the syndrome corresponding to trellis state σ .

The quantity $\gamma_\ell(\sigma', \sigma)$ is called the branch metric and is given by

$$\gamma_\ell(\sigma', \sigma) = \begin{cases} 1 - \delta & \text{if } (\sigma', \sigma) \in \mathcal{E}_\ell^{(0)} \\ \delta & \text{if } (\sigma', \sigma) \in \mathcal{E}_\ell^{(1)} \end{cases}.$$

The a posteriori LLRs computed via (5) are then used to make decisions on $\{d_i\}$ according to (4).

6 Experiments

6.1 Experimental setup

Experiment configuration and hyperparameters. We consider a cross-silo scenario with $n = 15$ clients (all participating in each training round) out of which n_m are malicious. The goal of the server is to prevent an attack by identifying the malicious clients and exclude their models from the global aggregation. The experiments are conducted for an image classification problem on the MNIST [32] and CIFAR-10 [33] datasets. For the MNIST dataset, we rely on a one-layer fully-connected neural network and for the CIFAR-10 dataset, we adopt a CNN instantiated as a ResNet-18 [34].

We assume that the server has a small validation dataset at its disposal to perform the group tests (the validation dataset is not used to do training). Such dataset is not required by FedGT, but is used

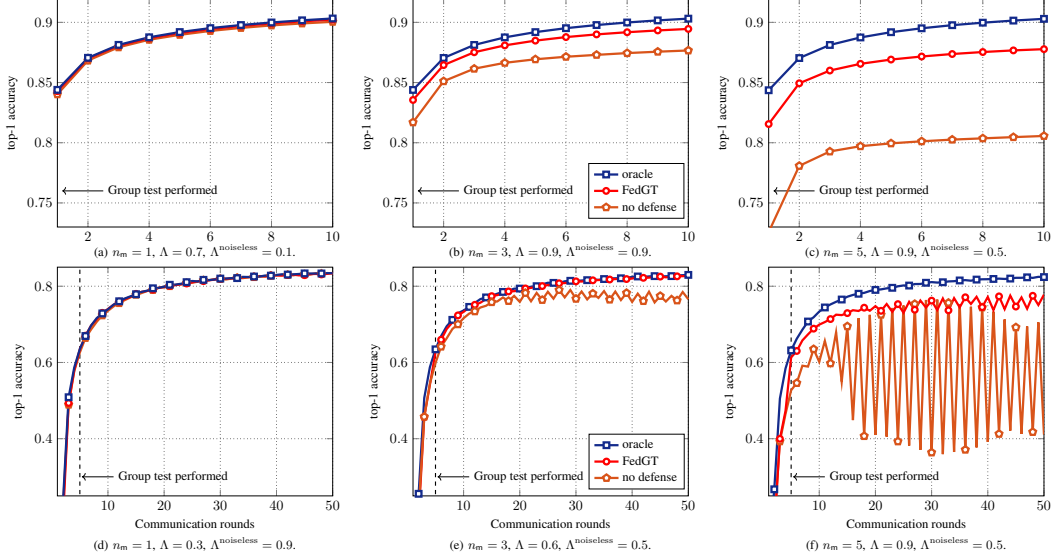


Figure 3: Average top-1 accuracy on the MNIST (row 1) and CIFAR10 (row 2) datasets for different number of malicious clients.

here due to our choice for the test in the experiments. The validation dataset should contain data that are sampled from a distribution close to the underlying distribution of the (benign) clients’ datasets, i.e., it should be a *quasi-dataset* [15, 17]. For the experiments, we create the validation dataset by randomly sampling 100 data-points from the training set, i.e., the label distribution may not be uniform. The remaining training data (of size 59900 for MNIST and size 49900 for CIFAR-10) are split evenly at random among the 15 clients. For MNIST, we use the cross-entropy loss and stochastic gradient descent with a learning rate of 0.01, batch size of 64, and number of local epochs equal to 1. For CIFAR-10, we use the cross-entropy loss and stochastic gradient descent with momentum and parameters taken from [1]: the learning rate is 0.05, momentum is 0.9, and the weight decay is 0.001. Furthermore, the batch size is set to 128 and the number of local epochs is set to 5. The results presented are averaged over 100 and 5 runs for MNIST and CIFAR-10, respectively.

We compare the performance of FedGT with two benchmarks: “no defense” and “oracle”. The no defense benchmark corresponds to the case of plain federated learning over all clients, i.e., disregarding some clients may be malicious, while the oracle assumes that the server knows the malicious clients and discards them.

To demonstrate the effectiveness of FedGT, we perform the group testing step only once during the training, constituting the weakest version of our framework. In particular, for MNIST, we perform a group test in the first round and for CIFAR-10, in the fifth round. We pick as the assignment matrix a parity-check matrix of a BCH code [35] of length 15 and redundancy 8, meaning that we create a group testing scheme where the 15 clients are pooled into 8 groups, each containing 4 clients (with this choice, FedGT ensures the same level of privacy as full secure aggregation with 4 clients).

Test. FedGT is general and can be applied to any test on the test groups. For example, a test may consider the accuracy as the metric of interest. Let v_i denote the measured metric on the aggregated model of test group i evaluated on the validation dataset and let $\mathbf{v} = \{v_1, v_2, \dots, v_m\}$. To determine whether a client is malicious or not, we consider a simple approach where

$$t_i = \begin{cases} 0, & v_i \geq \rho \cdot v^* \\ 1, & \text{otherwise} \end{cases}, \quad i \in [m], \quad (6)$$

where $0 \leq \rho \leq 1$ and $v^* = \arg \max_{i \in [m]} v_i$, i.e., test group is labeled as negative when the metric is close to the maximum value among the test groups. Thereafter, the test vector $\mathbf{t} = \{t_1, t_2, \dots, t_m\}$ is fed to a forward-backward decoder as described in Section 5.2 and $\hat{\mathbf{d}}$ is obtained. In the special case of $\hat{\mathbf{d}} = \mathbf{1}$, i.e., all clients are flagged as malicious, one may either cancel the learning procedure or, as done in the experiments, proceed without a defense. For all experiments, we use $\rho = 0.96$.

Distribution $Q(\mathbf{t}|s)$, prevalence δ , and threshold Λ . The decoder requires the distribution $Q(\mathbf{t}|s)$, the prevalence δ , and the threshold Λ . We model the noisiness of the test as $Q(\mathbf{t}|s) = \prod_{i=1}^m Q(t_i|s_i)$,

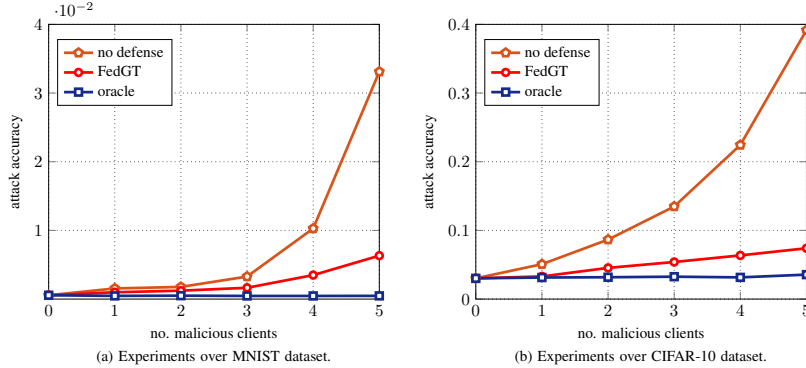


Figure 4: Average attack accuracy versus the number of malicious clients.

and $Q(t_i|s_i)$ as a binary symmetric channel (BSC), i.e., $Q(t_i|s_i) = 1 - p$ if $t_i = s_i$ and $Q(t_i|s_i) = p$ if $t_i \neq s_i$. We select $p = 0.05$. Further, in the experiments we feed the decoder the prevalence $\delta = n_m/n$. For the case of $n_m = 0$, we use a mismatched metric $\delta = 0.1$. Note that the true distribution $Q(t|s)$ is in general unknown and hard to estimate. Even assuming that the BSC is a good model, p is unknown. Moreover, n_m is unknown and, hence, so is the prevalence. Our empirical results show that FedGT is robust against a mismatch in the value of p and the prevalence δ used in the decoding stage. Finally, we evaluate for $\Lambda \in \{0.1, 0.2, \dots, 0.9\}$ and present the best result. Note that Λ is a design choice.

6.2 Experimental results for untargeted attacks

We consider a label permutation attack as the attacker’s untargeted strategy. The malicious devices have an offset of 1 to the labels of their data, i.e., the correct label 0 is changed to a 1, 1 to 2, up to 9 changed to a label 0. The attacker aims at damaging the classification accuracy as a whole, i.e., an attacker wants to lower the top-1 accuracy. For this reason, we use the top-1 accuracy on the test groups aggregates as the metric for the testing strategy adopted by the server.

In Fig. 1, we plot the top-1 accuracy versus n_m for MNIST (left) and CIFAR-10 (right). The top-1 accuracy is evaluated over the test dataset after 10 and 50 communications rounds for MNIST and CIFAR-10, respectively. When no defense is in place, a significant drop in accuracy is observed as the number of malicious clients grows. Remarkably, FedGT permits to identify malicious clients with low misdetection and false alarm probabilities, which translates into a high top-1 accuracy: For n_m up to 4, the top-1 accuracy of GTFed is within 1% of the performance of an oracle that allows to perfectly identify malicious clients for CIFAR-10 and within 2% for MNIST. For $n_m = 5$, i.e., a third of the clients are malicious, the performance of FedGT is only 5% worse than the oracle’s for CIFAR-10. Furthermore, numerically we observed that FedGT performs as good as plain federated learning when there are no malicious clients, i.e., $n_m = 0$ (FedGT does not harm the learning process if no malicious clients are participating if it does not trigger false alarms).

In Fig. 3, we plot the top-1 accuracy per communication round over MNIST (first row) and CIFAR-10 (second row) for $n_m \in \{1, 3, 5\}$. For $n_m = 1$, the attack is not very powerful, as the no defense and oracle benchmarks have similar performance. For $n_m = 3$ and $n_m = 5$, the impact on the top-1 accuracy of the attack is significant, as shown by the significant gap between the no defense and oracle curves. FedGT significantly closes this gap. We observe an interesting phenomenon for the experiments over the CIFAR-10 dataset. For $n_m = 3$ and 5, the no defense curve exhibits significant fluctuations throughout the rounds. Furthermore, as n_m increases, the peak distance of the fluctuations also increases. This instability can be attributed to the presence of a high number of malicious clients. Notably, although the performance of FedGT also fluctuates, it does so to a significantly lesser extent.

6.3 Experimental results for targeted attacks

We consider targeted data-poisoning, i.e., label-flipping attacks. We refer to the attacked label as the source label and the resulting label after the flip as the target label. For MNIST, we consider malicious clients to flip the source label 1 into the target label 7. As such, the objective of the malicious clients is to cause the global model to misclassify 1’s into 7’s. Similarly, for CIFAR-10, we consider a label flip attack where the malicious clients change the source label 4, i.e., horses, into the target label

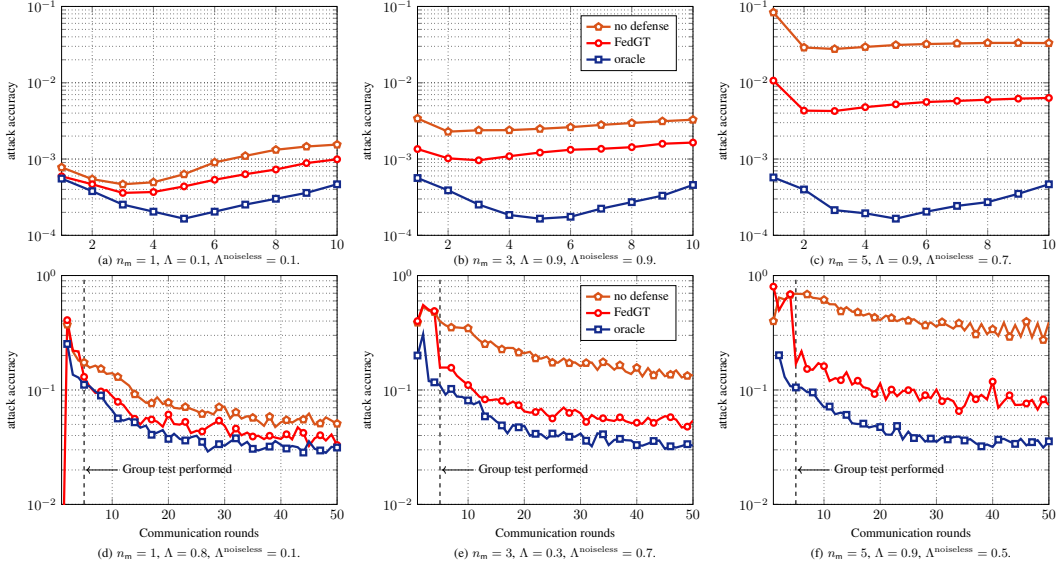


Figure 5: Average attack accuracy on the MNIST (row 1) and CIFAR10 (row 2) datasets for varying number of malicious clients.

7, i.e., deers. As the adversary objective is not to deteriorate the global model but only to make it misinterpret the source label as the target label, we adopt the *attack accuracy* as the metric of interest, defined as the fraction of source labels that are classified as the target label in the test dataset.

We consider the source label recall, i.e., the fraction of source labels that are classified into the correct label, as the performance metric adopted in the testing strategy to flag test groups containing malicious clients. Indeed, the group accuracies, adopted as the performance metric for untargeted attacks, are not distinguishable. This is expected as the attack does not notably impact the overall accuracy. Although we assume the server is informed of what label is under attack, we remark that it is straightforward to detect the labels under attack as the source label recall in a test group is significantly reduced in the presence of a malicious client.

In Fig. 4, we show the attack accuracy (evaluated over the test dataset) of FedGT. For experiments over MNIST dataset the attack we measure the attack accuracy after 10 communication rounds, while for experiments over CIFAR-10, we measure it after 50 rounds. We observe from Fig. 4a, that the $1 \rightarrow 7$ label flip does not have a big impact for $n_m \in [5]$ for MNIST, but experiments over CIFAR-10 show that a “horse” \rightarrow “deer” label flip attack has a huge impact (see Fig. 4b). FedGT is able to efficiently limit the impact of the attack even if 30% of the clients are malicious.

In Fig. 5, we demonstrate the label-flipping attack for $n_m = \{1, 3, 5\}$ over communication rounds. For MNIST, the attack impact is limited even for the case of no defense. However, even though the attack is weak, FedGT is able to identify the malicious clients and dampen the attack, e.g., after 10 communication rounds for $n_m = 5$, the attack accuracy is more than three times weaker by employing FedGT. On CIFAR-10, the impact of the attack is more significant. For example, for $n_m = 5$ after 50 communication rounds, an oracle-aided scheme has an attack accuracy of 3%, while the no defense strategy suffers an attack accuracy of 30 – 40%. Using FedGT, the attack accuracy can be reduced (with respect to no defense) to 7 – 8%, thus operating close to an oracle-aided strategy.

7 Conclusion

We proposed FedGT, a novel framework for identifying malicious clients in federated learning with secure aggregation. By grouping clients into overlapping groups, FedGT allows for a balance between privacy and security, providing improved identification capabilities at the expense of secure aggregation involving fewer clients. Extensive experiments for data-poisoning attacks demonstrate the effectiveness of FedGT in identifying malicious clients, resulting in high utility. To the best of our knowledge, this is the first work that provides a solution for identifying malicious clients in federated learning with secure aggregation. While not considered in this paper, our framework is also applicable against model-poisoning attacks provided proper group tests are available.

Acknowledgments and Disclosure of Funding

This work was partly funded by the German Research Foundation (DFG) under Grant Agreement No. WA 3907/7-1 and by the Swedish Research Council (VR) under grant 2020-03687.

References

- [1] H. B. McMahan, E. Moore, D. Ramage, S. Hampson, and B. Agüera y Arcas, “Communication-efficient learning of deep networks from decentralized data,” in *Proc. Int. Conf. Artificial Intell. Stats. (AISTATS)*, (Fort Lauderdale, FL), pp. 1273–1282, Apr. 2017.
- [2] M. Fredrikson, S. Jha, and T. Ristenpart, “Model inversion attacks that exploit confidence information and basic countermeasures,” in *Proc. ACM SIGSAC Conf. Comput. Commun. Secur. (CCS)*, (Denver, CO), pp. 1322–1333, Oct. 2015.
- [3] Z. Wang, M. Song, Z. Zhang, Y. Song, Q. Wang, and H. Qi, “Beyond inferring class representatives: User-level privacy leakage from federated learning,” in *Proc. IEEE Int. Conf. Comp. Commun. (INFOCOM)*, (Paris, France), pp. 2512–2520, May 2019.
- [4] K. Bonawitz, V. Ivanov, B. Kreuter, A. Marcedone, H. B. McMahan, S. Patel, D. Ramage, A. Segal, and K. Seth, “Practical secure aggregation for privacy-preserving machine learning,” in *Proc. ACM SIGSAC Conf. Comput. Commun. Secur. (CCS)*, (Dallas, TX), pp. 1175–1191, Nov. 2017.
- [5] J. H. Bell, K. A. Bonawitz, A. Gascón, T. Lepoint, and M. Raykova, “Secure single-server aggregation with (poly)logarithmic overhead,” in *Proc. ACM SIGSAC Conf. Comput. Commun. Secur. (CCS)*, (online), pp. 1253–1269, Nov. 2020.
- [6] G. Baruch, M. Baruch, and Y. Goldberg, “A little is enough: Circumventing defenses for distributed learning,” in *Annual Conference on Neural Information Processing Systems (NeurIPS)*, vol. 32, 2019.
- [7] V. Tolpegin, S. Truex, M. E. Gursoy, and L. Liu, “Data poisoning attacks against federated learning systems,” in *Computer Security – ESORICS 2020* (L. Chen, N. Li, K. Liang, and S. Schneider, eds.), (Cham), pp. 480–501, Springer International Publishing, 2020.
- [8] H. Wang, K. Sreenivasan, S. Rajput, H. Vishwakarma, S. Agarwal, J. yong Sohn, K. Lee, and D. S. Papailiopoulos, “Attack of the tails: Yes, you really can backdoor federated learning,” in *Annual Conference on Neural Information Processing Systems (NeurIPS)*, December 6–12 2020.
- [9] C. Fung, C. J. M. Yoon, and I. Beschastnikh, “Mitigating sybils in federated learning poisoning,” 2018.
- [10] M. Fang, X. Cao, J. Jia, and N. Z. Gong, “Local model poisoning attacks to byzantine-robust federated learning,” in *Proceedings of the 29th USENIX Conference on Security Symposium, SEC’20*, (USA), USENIX Association, 2020.
- [11] P. Blanchard, E. M. El Mhamdi, R. Guerraoui, and J. Stainer, “Machine learning with adversaries: Byzantine tolerant gradient descent,” in *Advances in Neural Information Processing Systems* (I. Guyon, U. V. Luxburg, S. Bengio, H. Wallach, R. Fergus, S. Vishwanathan, and R. Garnett, eds.), vol. 30, Curran Associates, Inc., 2017.
- [12] D. Yin, Y. Chen, K. Ramchandran, and P. Bartlett, “Byzantine-robust distributed learning: Towards optimal statistical rates,” 2018.
- [13] D. Cao, S. Chang, Z. Lin, G. Liu, and D. Sun, “Understanding distributed poisoning attack in federated learning,” in *the 25th International Conference on Parallel and Distributed Systems (ICPADS)*, 2019.
- [14] X. Cao, Z. Zhang, J. Jia, and N. Z. Gong, “Flcert: Provably secure federated learning against poisoning attacks,” *IEEE Transactions on Information Forensics and Security*, vol. 17, pp. 3691–3705, 2022.
- [15] X. Pan, M. Zhang, D. Wu, Q. Xiao, S. Ji, and M. Yang, “Justinian’s gaavernor: Robust distributed learning with gradient aggregation agent,” in *USENIX Security Symposium*, 2020.
- [16] X. Cao, M. Fang, J. Liu, and N. Z. Gong, “Fltrust: Byzantine-robust federated learning via trust bootstrapping,” 2020.

- [17] R. A. Mallah, D. Lopez, G. B. Marfo, and B. Farooq, “Untargeted poisoning attack detection in federated learning via behavior attestation,” 2021.
- [18] J. Park, D.-J. Han, M. Choi, and J. Moon, “Sageflow: Robust federated learning against both stragglers and adversaries,” in *Advances in Neural Information Processing Systems*, vol. 34, pp. 840–851, 2021.
- [19] P. Kairouz, H. B. McMahan, B. Avent, A. Bellet, M. Bennis, A. N. Bhagoji, K. Bonawit, and et al., “Advances and open problems in federated learning,” 2021.
- [20] R. Dorfman, “The detection of defective members of large populations,” *The Annals of Mathematical Statistics*, vol. 14, no. 4, pp. 436–440, 1943.
- [21] J. So, B. Güler, and A. S. Avestimehr, “Byzantine-resilient secure federated learning,” *IEEE Journal on Selected Areas in Communications*, vol. 39, no. 7, pp. 2168–2181, 2021.
- [22] K. Pillutla, S. M. Kakade, and Z. Harchaoui, “Robust aggregation for federated learning,” *IEEE Transactions on Signal Processing*, vol. 70, pp. 1142–1154, 2022.
- [23] Z. Zhang, J. Li, S. Yu, and C. Makaya, “Safelearning: Enable backdoor detectability in federated learning with secure aggregation,” 2021.
- [24] S. Li, E. C.-H. Ngai, and T. Voigt, “An experimental study of byzantine-robust aggregation schemes in federated learning,” *IEEE Transactions on Big Data*, pp. 1–13, 2023.
- [25] M. Aldridge, O. Johnson, and J. Scarlett, “Group testing: An information theory perspective,” 2019.
- [26] V. Shejwalkar, A. Houmansadr, P. Kairouz, and D. Ramage, “Back to the drawing board: A critical evaluation of poisoning attacks on production federated learning,” 2021.
- [27] A. R. Elkordy, J. Zhang, Y. H. Ezzeldin, K. Psounis, and A. S. Avestimehr, “How much privacy does federated learning with secure aggregation guarantee?,” *ArXiv*, vol. abs/2208.02304, 2022.
- [28] L. Bahl, J. Cocke, F. Jelinek, and J. Raviv, “Optimal decoding of linear codes for minimizing symbol error rate,” *IEEE Trans. Inf. Theory*, vol. 20, no. 2, pp. 284–287, 1974.
- [29] F. Kschischang, B. Frey, and H.-A. Loeliger, “Factor graphs and the sum-product algorithm,” *IEEE Trans. Inf. Theory*, vol. 47, no. 2, pp. 498–519, 2001.
- [30] J. Wolf, “Efficient maximum likelihood decoding of linear block codes using a trellis,” *IEEE Trans. Inf. Theory*, vol. 24, no. 1, pp. 76–80, 1978.
- [31] G. Liva, E. Paolini, and M. Chiani, “Optimum detection of defective elements in non-adaptive group testing,” in *Annu. Conf. Information Sciences and Systems (CISS)*, (Baltimore, MD), 2021.
- [32] Y. LeCun and C. Cortes, “MNIST handwritten digit database,” 2010.
- [33] K. He, X. Zhang, S. Ren, and J. Sun, “Deep residual learning for image recognition,” in *2016 IEEE Conference on Computer Vision and Pattern Recognition (CVPR)*, pp. 770–778, 2016.
- [34] A. Krizhevsky, V. Nair, and G. Hinton, “Cifar-10 (canadian institute for advanced research),” 2009.
- [35] R. Bose and D. Ray-Chaudhuri, “On a class of error correcting binary group codes,” *Information and Control*, vol. 3, no. 1, pp. 68–79, 1960.